Time Evolution of the Electronic Structure of $1T$-TaS_2 through the Insulator-Metal Transition

L. Perfetti,[1] P. A. Loukakos,[1] M. Lisowski,[1] U. Bovensiepen,[1] H. Berger,[2] S. Biermann,[3] P. S. Cornaglia,[3] A. Georges,[3] and M. Wolf[1]

[1]*Fachbereich Physik, Freie Universität Berlin, Arnimallee 14, 14195 Berlin, Germany*
[2]*Institut de Physique de la Matiére Complexe, EPFL, CH-1015 Lausanne, Switzerland*
[3]*Centre de Physique Theorique, École Polytechnique, 91128 Palaiseau Cedex, France*

(Received 16 May 2006; published 8 August 2006)

Femtosecond time-resolved photoemission is used to investigate the time evolution of electronic structure in the Mott insulator $1T$-TaS_2. A collapse of the electronic gap is observed within 100 femtoseconds after optical excitation. The photoemission spectra and the spectral function calculated by dynamical mean field theory show that this insulator-metal transition is driven solely by hot electrons. A coherently excited lattice displacement results in a periodic shift of the spectra lasting for 20 ps without perturbing the insulating phase. This capability to disentangle electronic and phononic excitations opens new directions to study electron correlation in solids.

DOI: 10.1103/PhysRevLett.97.067402 PACS numbers: 78.47.+p, 71.10.Fd, 71.30.+h, 79.60.Bm

Materials exhibiting photoinduced transitions from an insulating to a metallic character are ideal candidates for ultrafast optical switches because of their giant photoconductivity and ultrafast recovery time [1–4]. In typical systems of interest the insulating ground state is determined by either Mott or Peierls instabilities. While in a Mott insulator the electrons of a half-filled conduction band are localized due to their mutual repulsion, the electronic gap of a Peierls insulator arises from a periodic distortion of the lattice. The giant photoconductivity observed in both cases has been ascribed to a photoinduced insulator to metal transition [3–5]. Although the breakdown of the insulating phase is commonly accepted, a direct evidence for the collapse of the electronic gap and the respective time scale is lacking up to date. Moreover, it is still debated whether this transition is driven directly by the excited electrons or by the subsequent rearrangement of the nuclear lattice [1–5].

A conclusive answer to this question requires tools that probe the nuclear and the electronic structure under nonequilibrium conditions. On one hand, femtosecond time-resolved x-ray diffraction monitors the nuclear lattice directly [6] and provides clear indication that phonons drive the insulator-metal transition in the Peierls insulator VO_2 [1,2,7]. Femtosecond time-resolved photoemission, on the other hand, probes the temporal evolution of the electronic states. Thus, this technique provides direct access to the collapse of the electronic gap.

In this Letter, we show by time-resolved photoemission spectroscopy and by dynamical mean field theory (DMFT) that in the Mott insulator $1T$-TaS_2 the breakdown of the electronic energy gap around the Fermi level arises from a purely electronic process. A pronounced response of the lattice due to a coherent nuclear displacement can be clearly identified and is properly disentangled from the effect of the excited electrons. We demonstrate that such coherent phonons modulate the binding energy of the electronic states, but are not responsible for the insulator to metal transition.

The layered compound $1T$-TaS_2 is a quasi-two-dimensional crystal without surface reconstruction [8]. In this system, both electron-electron and electron-phonon interactions are important. The strong coupling between valence electrons and phonons periodically distorts the lattice, modifying the spatial distribution of the charge density. As sketched in Fig. 1(a), the structural unit in the Ta plane consists of ''stars'' with a central atom and two rings with 6 Ta atoms each [8,9]. The formation of these metal clusters is accompanied by a charge density wave (CDW), namely, a large charge transfer from the outer ring towards the inner part of the stars [10]. Since Ta atoms have nominal d^1 valence, only 6 orbitals of the cluster are totally occupied whereas the 7th is half filled [11]. Figure 1(b) shows that the electronic bands split into 2 occupied manifolds (each embedding 3 orbitals), and a conduction band arising from the uppermost cluster orbital (UCO). According to experiments [12,13], the CDW amplitude increases at low lattice temperature T_l, thus reducing the overlap between orbitals of different clusters. At the critical value of $T_l = 180$ K, the energy U that is necessary for the double occupation of one UCO becomes larger than the bandwidth W. Therefore, the metallic state is no longer stable and electrons localize into the Mott insulating (MI) phase [14,15].

Angle resolved photoelectron spectroscopy (ARPES) is highly sensitive to the different electronic structures across the metal-insulator transition [13]. Therefore, we first discuss the photoemission signal generated by 6 eV probe photons while the sample is in thermal equilibrium. The ARPES spectra of Fig. 1(c) have been recorded in normal emission (parallel wave vector $k_\parallel = 0 \pm 0.02$ Å^{-1}) in the metallic (room temperature) and insulating phase (lattice temperature $T_l = 30$ K). These spectra are similar to measurements performed at $\simeq 20$ eV photon energy, where the

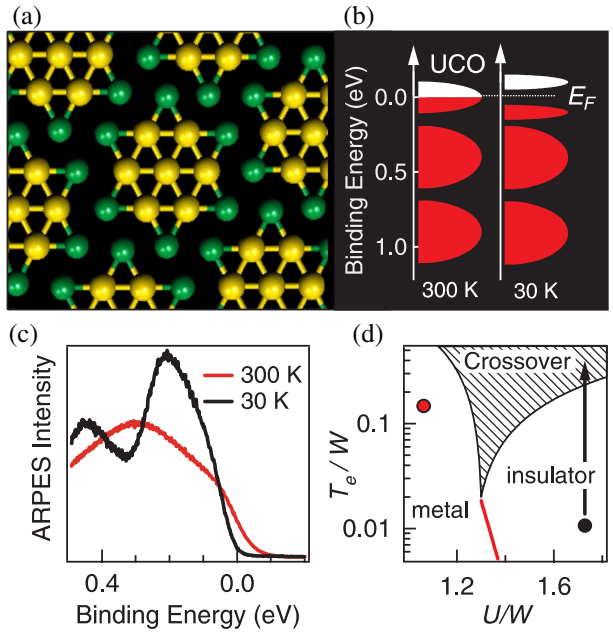

FIG. 1 (color online). (a) The in-plane CDW distortion produces "stars" of Ta atoms in which the per atom electronic density is larger towards the center (yellow) and smaller towards the periphery (green). (b) Sketch of the electronic states with the uppermost cluster orbital (UCO) band in the metallic (T_l = 300 K) and Mott phase (T_l = 30 K). (c) Normal emission spectra acquired at 300 K (red curve) and T_l = 30 K (black curve). (d) Phase diagram of a Mott transition in the U/W, T_e/W plane as obtained from the Hubbard model [Eq. (1)]; U is the Coulomb repulsion, W is the bandwidth. Notice that in thermal equilibrium $T_e = T_l$ whereas out of equilibrium $T_e \gg T_l$. The shaded area is a crossover phase between the metallic and Mott phase whereas the red line delimits a first order transition. Red and black circles indicate U/W values for T_l = 300 K and T_l = 30 K, respectively. The black arrow shows the large increase of T_e induced by the absorption of the pump pulse.

direct photoemission outweighs secondary electrons and the sudden approximation is safe. In agreement with Ref. [16], we also conclude that 6 eV probe photons provide spectra that are roughly proportional to the electronic spectral function. The spectral function contains all information about the dispersion of electronic states and many-body interactions. As an example, the room temperature spectrum of Fig. 1(c) displays the Ta d band cut by the Fermi-Dirac distribution. Upon cooling to 30 K, a large amount of the spectral weight moves from the Fermi level to the lower Hubbard band at $U/2 \simeq 0.21$ eV, leading to the opening of the electronic gap. Figure 1(d) indicates the estimated U/W ratio when the system is at room temperature (metal) and at 30 K (insulator). This phase diagram can be extended to the nonequilibrium case if the photoexcitation produces a quasithermal distribution of electrons with temperature $T_e \gg T_l$.

In the following we investigate nonequilibrium states by means of time-resolved ARPES [17]. The sample is excited by a 50 fs pump pulse with center energy of 1.5 eV while the photoelectrons are generated by a delayed 80 fs probe pulse with energy of 6 eV [17]. We estimate that the pump pulse excites $\simeq$0.1 electrons in each star. Figure 2(a) shows several time-resolved ARPES spectra acquired at room temperature, at different pump-probe delays. The excited distribution tail indicates that electrons reach an energy density which is equivalent to an electronic temperature [18] of $T_e \simeq 1100$ K. Their fast relaxation is shown in Fig. 2(b), where a color scale image maps the photoelectron intensity as a function of binding energy and pump-probe delay. Electrons release their energy to the lattice on a time scale τ_M = 150 fs, thus providing evidence for an efficient electron-phonon coupling. However, the large heat capacity of the phonon bath limits the increase of the lattice temperature to 30 K. This cooling process is typical of metals and is usually described by the two temperature model [19].

If the system is originally in the MI phase, the photoexcitation does not merely act as a redistribution of the electronic occupation. As shown by the phase diagram of Fig. 1(d), the elevated T_e induces an ultrafast transition towards the crossover phase residing between the insulator and the metal. According to the Hubbard model, the crossover phase differs from the metallic one because it does not display bandlike quasiparticles near the Fermi level but rather "incoherent" midgap states. This process is captured by the time-resolved spectra of Fig. 3(a), which display a major transfer of the spectral weight from the Hubbard band to the originally gapped region near the Fermi level. The instantaneous collapse (<100 fs) and subsequent recovery of the MI phase is monitored by the peak intensity $I_H(\tau)$ of the Hubbard band. Figure 3(b) shows that $I_H(\tau)$ drops suddenly to 80% of the original value and recovers its intensity with time constant of τ_H = 680 fs. Therefore, the Mott insulator is soon reestablished by the cooling of excited electrons. A closer inspection of Fig. 3(a) reveals that nonequilibrium spectra display also a shift of the Hubbard peak towards the Fermi level. The

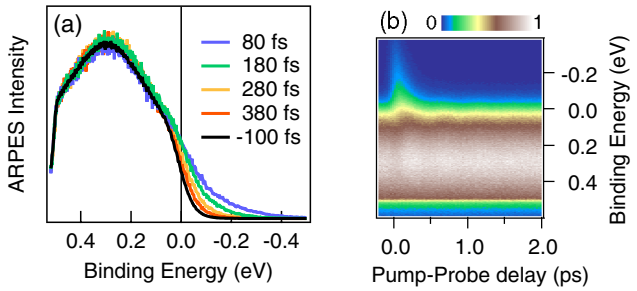

FIG. 2 (color online). (a) Spectra acquired in the metallic phase (T_l = 300 K) at different pump-probe delays. (b) Photoelectron intensity map as function of pump-probe delay and binding energy (T_l = 300 K).

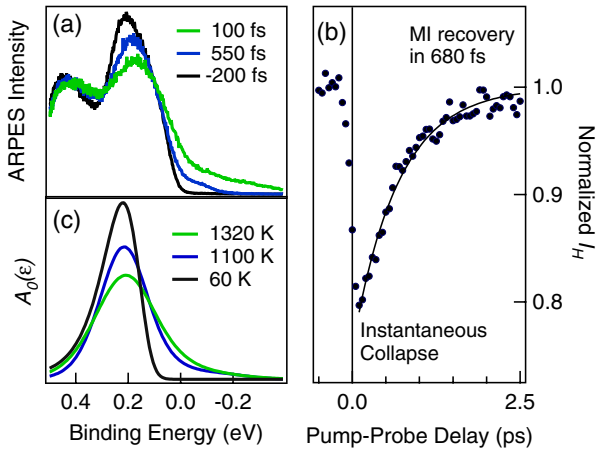

FIG. 3 (color online). (a) Spectra acquired at $\tau = 100$ fs (green curve) and $\tau = 550$ fs (blue curve) are compared to the spectrum collected before the arrival of the pump pulse (black curve). Although T_e reaches high values, the lattices temperature remains roughly at 30 K. (b) Time-resolved ARPES intensity of the Hubbard peak normalized to the equilibrium value. The exponential fit (black line) provides the decay time $\tau_H = 680$ fs. (c) Spectral function of the Hubbard model calculated at the center of the Brillouin zone for $U = 0.4$ and $W = 0.29$ eV. The electronic temperature and filling factor are $T_e = 1350$ K, $n = 0.48$ (green curve), $T_e = 1100$ K, $n = 0.49$ (blue curve), $T_e = 60$ K, $n = 0.5$ (black curve).

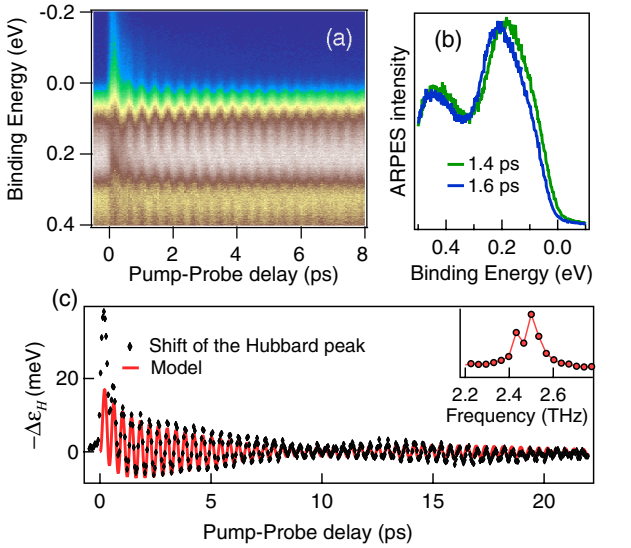

FIG. 4 (color online). (a) Photoelectron intensity map measured in the MI phase ($T_l = 30$ K) as a function of pump-probe delay and binding energy. (b) Two spectra acquired on a maximum ($\tau = 1.4$ ps) and minimum ($\tau = 1.6$ ps) of one CDW oscillation period display a rigid shift with respect to each other. (c) Measured shift of the Hubbard peak (diamonds) and the calculated $gX(\tau)$ (solid line). The inset displays the Fourier transform of the oscillations as a function of frequency.

shift arises from photoinduced doping, inasmuch as the nonequilibrium occupation of the UCO deviates from half filling. We perform a numerical simulation of the spectra in order to estimate the effective temperature of the electrons and the UCO filling factor n after excitation. The UCO band and its correlation energy are described by the Hubbard model:

$$H_e = -t \sum_{\langle i,j\rangle,\sigma} (c^\dagger_{i,\sigma} c_{j,\sigma} + c^\dagger_{j,\sigma} c_{i,\sigma}) + U \sum_i n_{i,\uparrow} n_{i,\downarrow}, \qquad (1)$$

where $c_{i,\sigma}$ and $c^\dagger_{i,\sigma}$ are the destruction and creation operators of an electron at site i and with spin σ, $n_{i,\sigma} = c^\dagger_{i,\sigma} c_{i,\sigma}$ the occupation operator, t is the hopping matrix element between nearest neighbors, and $U = 0.4$ eV is the UCO Coulomb repulsion. Figure 3(c) plots the spectral function calculated with dynamical mean field theory [20] for suitable T_e and filling factor n. The best agreement to the spectrum measured at $\tau = 100$ fs is obtained for $T_e = 1320$ K and $n = 0.48$. It follows that the electronic temperature exceeds the MI stability range of Fig. 1(d), whereas n decreases by only a few percents. This finding proves that the elevated T_e dominates the breakdown of the Mott insulator.

Besides the ultrafast collapse of the MI phase, we also observe periodic modulation of the time-resolved ARPES spectra. The intensity map of Fig. 4(a) shows that large oscillations of the electronic spectra start abruptly at zero delay and endure for many picoseconds. The period of these oscillations corresponds closely to the breathing mode of the stars, also called the amplitude mode of the CDW [21]. In the cluster picture of Fig. 1(a), the short pump pulse transfers part of the electronic density towards the outer ring of the stars, leading to the displacement of the nuclear coordinate of the CDW amplitude mode. This collective and coherent excitation of the clustered atoms initiates a spectral oscillation of the coupled electronic states. We exploit the different response time of electrons and phonons to disentangle their contribution to the measured spectra. One picosecond after the absorption of the pump pulse, the electrons have already cooled down, and only the nuclear motion persists. The latter acts on the electronic structure in a remarkably simple way. Figure 4(b) compares the spectra acquired on a maximum and minimum of an oscillating period, at $\tau = 1.2$ ps and 1.6 ps, respectively. The two spectra display a rigid shift of 18 meV, proving that the oscillation of the CDW amplitude changes the mean binding energy of the lower Hubbard band without perturbing the Mott phase. Similar modulations of the binding energy are expected whenever phonons or magnons are strongly coupled to the electrons. The dynamics is analyzed by plotting in Fig. 4(c) the shift $-\Delta\varepsilon_H(\tau)$ of the lower Hubbard peak as a function of the pump-probe delay. Two modes with frequency $\nu_B = 2.45$ THz and $\nu_S = 2.51$ THz generate a beating response that decays with a time constant of $\tau_C = 9.5$ ps. The frequency ν_B is in excellent agreement with the bulk CDW oscillations measured by transient reflectivity [21]

whereas the ν_S response is attributed to the stiffer mode of the surface layer. Its amplitude appears 2 times larger than the bulk component due to the surface sensitivity of the photoelectron signal. The temporal evolution of the nuclear displacement $X_\alpha(\tau)$ is obtained [22] by the differential equation

$$\frac{\partial^2 X_\alpha}{\partial \tau^2} - \frac{\pi}{\tau_C}\frac{\partial X_\alpha}{\partial \tau} + (2\pi\nu_\alpha)^2 X_\alpha = F(\tau), \qquad (2)$$

where the suffix α stands for the displacement of the surface or bulk mode, $F(\tau)$ is the driving force, and τ_C is the damping time provided by anharmonic interaction with other phonons. The driving force is modeled with an exponential function having the decay time τ_H of the excited electronic state. We introduce the parameter g to quantify the coupling of UCOs electrons with the CDW displacement. Since the electronic bandwidth is much larger than the phonon frequencies, the electron-phonon Hamiltonian [23] reduces to the adiabatic limit $H_p = gX_\alpha \sum_{i,\sigma} n_{i,\sigma}$. Notice that X_α does not depend on the site i because the excitation occurs coherently in all stars. Consequently, X_α generates a deformation field g/e that shifts the electronic binding energy around the equilibrium value. Upon weighting the surface and bulk contribution to the spectra, the phonon induced shift of the Hubbard peak assumes the form $gX = g(c_S X_S + c_B X_B)$. Figure 4(c) compares the experimental data to $gX(\tau)$ calculated for $c_S = 0.65$, $c_B = 0.35$, and $\tau_H = 680$ fs. The model is in excellent agreement for $\tau > 1$ ps but does not reproduce the initial rise of $-\Delta\varepsilon_H(\tau)$. As depicted in Fig. 3(a) and 3(c), the Hubbard peak at early delays exhibits an additional, nonoscillating shift that arises from photoinduced doping.

In conclusion, photoexcitation of the Mott insulator $1T$-TaS_2 induces an insulator to metal transition and the excitation of a coherent phonon mode. Time-resolved photoelectron spectroscopy is employed to directly measure the time evolution of the electronic structure. The different response-time of electronic and nuclear excitation allows for an identification of the respective contributions to the measured spectra. (i) We observe the ultrafast collapse and 680 fs revival of the electronic gap after the absorption of the pump pulse. The spectral properties of the nonequilibrium state indicate a dominant contribution of the elevated electronic temperature and minor effects of photoinduced doping. Our results establish the primary process leading to the giant and fast photoresponse of Mott insulators. (ii) We prove that coherent excitation of phonons modulates the binding energy of the electrons around the equilibrium value. We propose that all coherently excited nuclear or spin excitations that are strongly coupled to the electrons may generate similar oscillations. Therefore, the nonequilibrium dynamics of electronic states observed by time-resolved ARPES open a novel and appealing direction for research in the field of highly correlated materials. Future experiments involving high temperature superconductors may provide new insights to the pairing mechanism.

We are grateful to Roberto Merlin for fruitful discussions. This project has been sponsored by the Deutsche Forschungsgemeinschaft, the Alexander von Humboldt Foundation, and the European Community which supported P. A. L. through Contract No. MEIF-CT-2003-501826.

[1] A. Cavalleri, Cs. Tóth, C. W. Siders, J. A. Squier, F. Ráksi, P. Forget, and J. C. Kieffer, Phys. Rev. Lett. **87**, 237401 (2001).
[2] A. Cavalleri, Th. Dekorsy, H. H. W. Chong, J. C. Kieffer, and R. W. Schoenlein, Phys. Rev. B **70**, 161102 (2004).
[3] S. Iwai, M. Ono, A. Maeda, H. Matsuzaki, H. Kishida, H. Okamoto, and Y. Tokura, Phys. Rev. Lett. **91**, 057401 (2003).
[4] M. Chollet *et al.*, Science **307**, 86 (2005).
[5] M. Fiebig, K. Miyano, Y. Tomioka, and Y. Tokura, Science **280**, 1925 (1998).
[6] K. Sokolowski-Tinten *et al.*, Nature (London) **422**, 287 (2003).
[7] S. Biermann, A. Poteryaev, A. I. Lichtenstein, and A. Georges, Phys. Rev. Lett. **94**, 026404 (2005).
[8] Ju-Jin Kim *et al.*, Phys. Rev. Lett. **73**, 2103 (1994).
[9] A. Yamamoto, Phys. Rev. B **27**, 7823 (1983).
[10] H. P. Hughes and J. A. Scarfe, Phys. Rev. Lett. **74**, 3069 (1995).
[11] K. Rossnagel and N. V. Smith, Phys. Rev. B **73**, 073106 (2006).
[12] L. Perfetti *et al.*, Phys. Rev. B **71**, 153101 (2005).
[13] L. Perfetti *et al.*, Phys. Rev. Lett. **90**, 166401 (2003); S. Colonna *et al.*, Phys. Rev. Lett. **94**, 036405 (2005).
[14] P. Fazekas and E. Tosatti, Philos. Mag. B **39**, 229 (1979).
[15] F. J. Di Salvo, J. A. Wilson, B. G. Bagley, and J. V. Waszczak, Phys. Rev. B **12**, 2220 (1975).
[16] J. D. Koralek *et al.*, Phys. Rev. Lett. **96**, 017005 (2006).
[17] M. Lisowski *et al.*, Phys. Rev. Lett. **95**, 137402 (2005).
[18] T_e is defined as the temperature of a thermalized electronic distribution with the same excess energy of the observed, nonequilibrium one.
[19] P. B. Allen, Phys. Rev. Lett. **59**, 1460 (1987).
[20] A. Georges *et al.*, Rev. Mod. Phys. **68**, 13 (1996).
[21] J. Demsar *et al.*, Phys. Rev. B **66**, 041101 (2002).
[22] R. Merlin, Solid State Commun. **102**, 207 (1997).
[23] S. Ciuchi and F. de Pasquale, Phys. Rev. B **59**, 5431 (1999); S. Fratini and S. Ciuchi Phys. Rev. B **72**, 235107 (2005).